Available online at www.sciencedirect.com

SciVerse ScienceDirect

Ceramics International 38 (2012) 2145–2151

CERAMICS INTERNATIONAL

www.elsevier.com/locate/ceramint

Characterization of porosity and defect imaging in ceramic tile using ultrasonic inspections

Elif Eren [a], Semra Kurama [a,*], Igor Solodov [b]

[a] Anadolu University, Faculty of Engineering and Architecture, Department of Materials Science and Engineering, Iki Eylul Campus, 26555 Eskisehir, Turkey
[b] Universität Stuttgart, Institut für Kunststofftechnik (IKT-ZfP), Pfaffenwaldring 32, 70569 Stuttgart, Germany

Received 17 August 2011; received in revised form 18 October 2011; accepted 20 October 2011
Available online 25 October 2011

Abstract

In this study, three different ultrasonic nondestructive methods (NDT) used to characterize porosity and identify defects in ceramic materials were employed as alternative approaches to conventional systems. A contact ultrasound technique, based on the A-scan, and measurements of the material frequency response were found to be useful for the characterization of porosity in porcelain tiles. Ceramic specimens with two types of simulated defects (a piece of paper and aluminum foil) were prepared and studied. The defects were readily identified in the ultrasonic A-scan and the location depth was measured. The technique, based on air-coupled ultrasound, was shown to be applicable for non-contact detection and imaging of defects in ceramic tiles.

Keywords: B. Defects; B. Porosity; D. Porcelain; Ultrasonic non-destructive technique

1. Introduction

Nondestructive techniques have been generally used for the detection of macroscopic defects in structures after they have been in service for some time. Nowadays, it has become increasingly evident that it is also practical and cost effective to expand the role of nondestructive evaluation to include all aspects of materials production and application. Therefore, current efforts are directed at developing and perfecting this technique in the controlling and monitoring of the materials production process [1].

Ultrasonic testing is a versatile NDT method which is applicable to most materials, metallic or non-metallic [2]. The ultrasonic test has been generally used for detecting internal flaws in steel materials, steel sheets or plates, welded portions, machine parts and other articles. Recently, the ultrasonic test has also been used to detect internal flaws in ceramics and new materials. However, conventional ultrasonic testing ascertains the condition of a detected flaw of a test article by estimating its size from the size of the echo reflected from the flaw and measured by means of an oscilloscope or suchlike. Alternatively, estimating the size of the defect is implemented using the size of a two-dimensional indication of the flaw detected by automatically scanning the test article [3].

There are different types of ultrasonic scanning approaches, such as the A-scan, the B-scan and the C-scan [4]. Ultrasonic echoes can be displayed as seen on an ordinary oscilloscope. The *X*-axis represents the time of flight of the pulses converted into the distance travelled by the pulses (depth of penetration). The deflection parallel to the *Y*-axis represents the amplitude of the echoes. This type of presentation is called an 'A-scan'. It shows a situation with the probe stationary in one position. An A-scan presentation is still the most used mode of display in ultrasonic testing [2]. The A-scan format provides a quantitative display of signal amplitude and time-of-flight data obtained at a single point on the surface of the test piece. The A-scan display can be used to analyze the type, size and location (mainly depth) of flaws [4].

Since the information that is available in an A-scan is basically one dimensional, interpretation with accompanying sketches and calculation is required to characterize the flaw. Imaging systems, using automated probe movement control

* Corresponding author. Tel.: +90 222 321 3550x6346; fax: +90 222 323 9501.
E-mail addresses: skurama@anadolu.edu.tr, semra.kurama@gmail.com (S. Kurama).

0272-8842/$36.00
doi:10.1016/j.ceramint.2011.10.056

and computerized data analysis and storage, greatly enhance the quality of defect characterization and ease of communication. There are basically two imaging techniques widely used in ultrasonic testing of components. These are the B-scan and the C-scan. In the B-scan display, the *Y*-axis is used in a different way. When moving the transducer along a straight line on the surface of the test object, the displacement of the transducer can be converted into an electrical signal (voltage) by a potentiometer and used to shift the spot on the oscilloscope screen. This dimension is normally displayed along the *X*-axis and the path of the ultrasonic pulse in the object is represented by the time base moving the spot in the *Y*-direction (usually from the top downwards). The B-scan presentation gives a cross-sectional view of the part being tested and shows the length and depth of a flaw in the test material. In some testing problems the depths of defects are irrelevant, but their distribution parallel to the test surface is an important feature. For this purpose, the presentation is rotated by 90°, such that the *X* and *Y*-direction are now both in the plane of the surface of the test object, i.e., the plane of scan. This type of display is called a 'C-scan' [2]. Alternatively, a C-scan format provides a semi-quantitative or quantitative display of signal amplitudes obtained over an area of the test piece surface. This information can also be used to map out the position of flaws on a plan view of the test piece. Additionally, a C-scan records time-of-flight data, which can be converted and displayed by image-processing equipment to provide an indication of flaw depth [4].

The quality control of porcelain tiles is important for the avoidance of defects during manufacturing and processing. However, the control of physical properties (such as porosity and water absorption) using traditional methods of quality control is extremely difficult. Recent studies show that the reliability of ceramic materials can be enhanced by an accurate rejection of products that contain critical defects. Three main flaws, currently found in ceramic, are cracks, porosity, and inclusions: density and structural variations may also greatly impair component performance in particular situations. The quality control of the sintered material was therefore achieved by means of ultrasonic imaging allows defect detection [5]. By starting from this point of view, in this study three different ultrasonic approaches were applied for the characterization of porosity, detection and imaging of different types of defect in ceramic materials.

2. Experimental

Standard porcelain tile granules were prepared using the uniaxial pressing technique in a 50 mm × 100 mm rectangular die at 450 kg/cm^2. Additional materials (paper and aluminum foil) were added to the system to simulate defects in the tiles. The tiles were numbered Tile 1, Tile 2 and Tile 3 according to their defect type. Tile 1 contained 1 cm^2 aluminum foil, Tile 2 contained 1 cm^2 paper and Tile 3 contained no defects. After the samples were dried at 110 °C, sintering of the tiles was carried out in a laboratory kiln (Nabertherm LS 12/13) at target temperatures (1200 °C for defective tiles and 1140 °C for porous tile with an industrial fast-firing cycle) for 46 min including cooling.

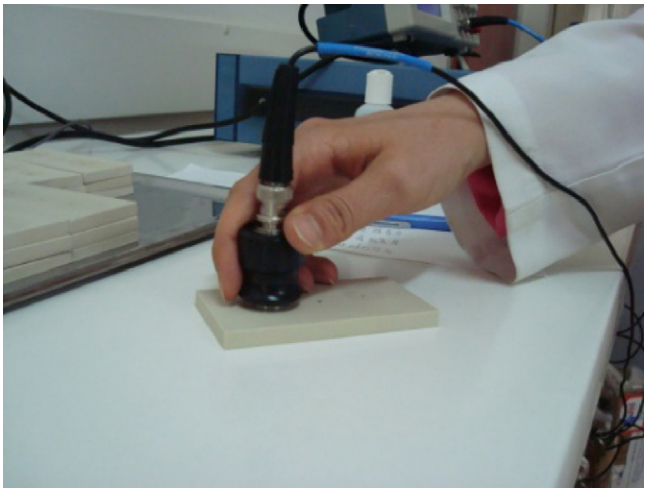

Fig. 1. The experimental set up for ultrasonic analysis.

An Olympus Panametrics-NDT Model 5800 Computer Controlled Pulser/Receiver was used for an ultrasonic time of flight measurement. The experimental set up of the ultrasonic analyses used is shown in Fig. 1. The time of flight of the ultrasonic waves (longitudinal waves) was measured using a 0.5 in. diameter contact ultrasonic transducer operating in pulse-echo mode. The center frequency of the transducer was 5 MHz. Silicone oil was used as a couplant material. The transit time was determined to an accuracy of ±40 ns. For each of the samples, the time of flight of the ultrasonic wave measurements were repeated 10 times. The thickness of the samples was measured using a micrometer. The velocity of the wave as it travelled through the material was determined by formula [6]:

$$V = \frac{2 \times d}{t} \quad (1)$$

where V is the velocity of the wave (m/s); d is the sample thickness (m); t is the arrival time between the front and back reflection (s).

To compare ultrasonic methods and the traditional method (Archimedes technique) results, the density and porosity of the tiles were measured.

3. Results and discussion

The bulk density, apparent density, apparent porosity and water absorption of the samples were measured using the Archimedes technique. In addition, the longitudinal velocity of each of the specimens was measured using the ultrasonic contact method. The density, porosity and water absorption values of the samples, measured by traditional methods, are given in Table 1. Results show that Tile 3 has a higher porosity than the others (Tile 1and Tile 2) due to its lower sintering temperature (1140 °C). Therefore, the first part of the study was achieved by preparing tiles with different types of defect.

Table 1
Change in bulk density, apparent density, apparent porosity and water absorption in the specimens studied.

Sample	Bulk density (g/cm^3)	Apparent density (g/cm^3)	Apparent porosity (%)	Water absorption (%)
Tile 1	2.359	2.360	0.065	0.027
Tile 2	2.367	2.368	0.033	0.014
Tile 3	2.326	2.440	4.690	2.017

3.1. Ultrasonic characterization of tiles

3.1.1. A-scan results

In the second part of the study, the tiles were analyzed using ultrasonic A-scans. The ultrasonic velocity values measured are given in Table 2.

Fig. 2 shows the ultrasonic velocity values in the tiles. The ultrasonic velocities in the defective parts of the tiles (Tile 1 and Tile 2), within the standard deviation, are the same as those for the intact areas of the specimens (Table 2). However, the time of flight in the porous sample (Tile 3) is substantially greater so that the ultrasonic velocity is about 20% lower than for Tiles 1 and 2. This result is an obvious consequence of the lower stiffness of the porous material sintered at lower temperature. It demonstrates that the measurements of ultrasonic velocity are a reliable tool for the characterization of porosity in ceramic materials.

On the other hand, the ultrasonic velocity of Tile 2 is slightly higher than that of Tile 1. This can be explained by the bulk density differences between the two tiles. As a result of the increased bulk density and the decreased porosity, Tile 2 has a somewhat higher ultrasonic velocity than Tile 1. Although both tiles were sintered at the same time and temperature in the kiln, differences in bulk densities between them were observed due to the inhomogeneities in sintering conditions and the pressing of the tiles.

In order to determine the feasibility of ultrasonic detection of the defects, the specimens with defects (Tiles 1 and 2) and porous sample (Tile 3) were inspected by using A-scan and C-scan presentations. Fig. 3(a) shows a typical ultrasonic A-scan measured in an intact part of Tile 1 containing a piece of aluminum foil. The time of flight for the defect-free part is determined by the signals successively reflected from the bottom plane of the specimen and is measured to be $T_1 = 2.6$ μs. A typical A-scan, obtained in the area of the defect, is given in Fig. 3(b). In this case, the pulses of maximum amplitude are also caused by bottom reflections, so that the time of flight measured using them is the same as that for the intact area of the specimen. The strong bottom reflections are due to the fact that the size of the aluminum foil defect is smaller than the diameter of the transducer and the transducer also collects the waves propagating outside the defect area.

The signals reflected from the defect are also seen in Fig. 3(b) and can be used for determining the depth of the defect position. The difference in times of flight between the signal

Table 2
Ultrasonic velocity values of samples.

Sample	Inspected part	Time of flight (μs)	Thickness (mm)	Ultrasonic velocity (m/s)
Tile 1	Defect-free	2.62 ± 0.03	7.25 ± 0.05	5550 ± 50
	Defective	2.6	7.23	5560
Tile 2	Defect-free	2.55 ± 0.04	7.12 ± 0.08	5600 ± 50
	Defective	2.54	7.13	5600
Tile 3	Defect-free	3.20 ± 0.04	7.20 ± 0.01	4500 ± 50

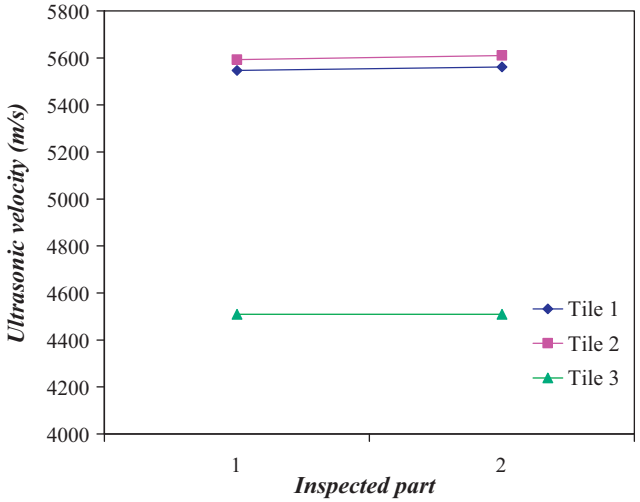

Fig. 2. Ultrasonic velocity of inspected parts of Tile 1, Tile 2 and Tile 3 (on the *X*-axis; 1 indicates defect-free parts, whereas 2 corresponds to defect areas in Tiles 1, 2 and arbitrary measurement position in Tile 3).

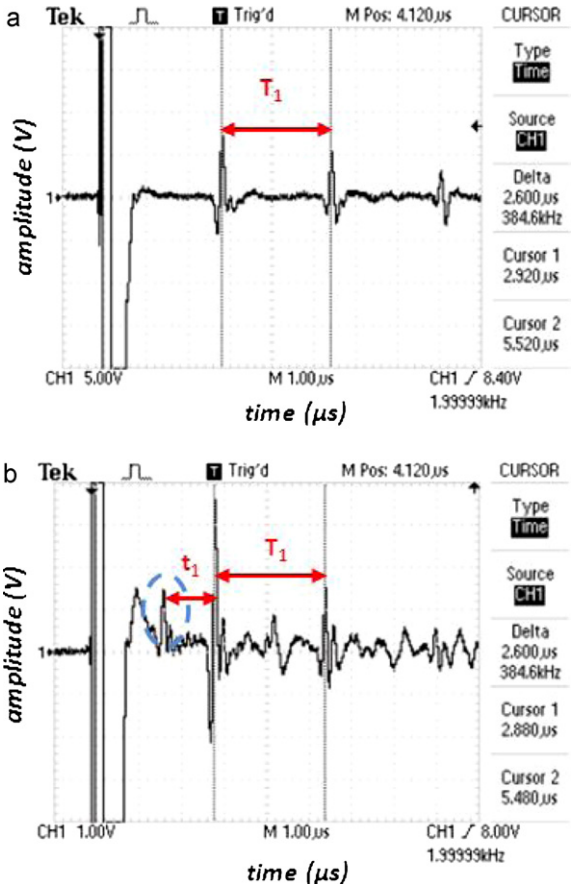

Fig. 3. Ultrasonic A-scan in: (a) a defect-free part, (b) the defect area of Tile 1.

reflected from the defect and the backwall echo is measured as $t_1 = 1.2$ μs in Fig. 3(b). Therefore, the defect position is 3.3 mm beyond the bottom plane of the specimen.

The amplitude of the signal reflected from the defect in an A-scan is determined by the difference in acoustic impedance between the intact material and the material of the defect as well as the size of the latter. For a constant input voltage, the reflection of an ultrasonic wave by the defect reduces the transmitted wave signal. Therefore, the ratio of the signal

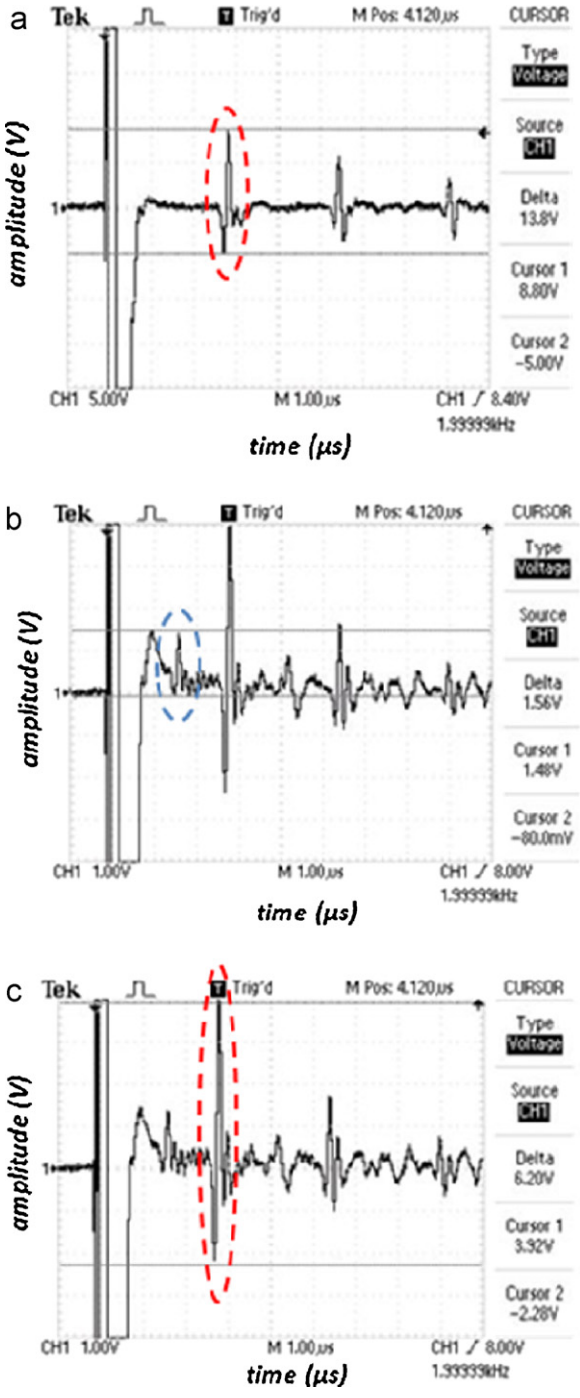

Fig. 4. Measurement of: (a) the amplitude of the backwall echo of the defect-free part, (b) ultrasonic echo reflected from the defect, (c) backwall echo in defected area of Tile 1.

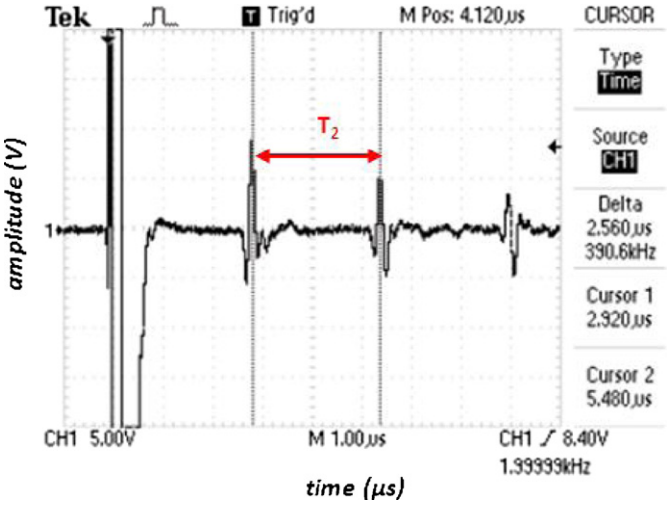

Fig. 5. Time of flight measurement in defect-free part of Tile 2.

reflected by the defect to the backwall echo characterizes the severity of the defect. Alternatively, it can also be characterized by a reduction of the amplitude of the backwall echo in the intact specimen and the one transmitted through the defect [7].

By comparing the data in Fig. 4, one can see that in Tile 1 the amplitude of the backwall echo reduces by about twice, from 13.8 V in the intact specimen (Fig. 4(a)) to 6.2 V in the defect area (Fig. 4(c)). The signal reflected from the aluminum foil defect in Tile 1 is measured at 1.56 V (Fig. 4(b)).

Fig. 5 represents a typical transmitted ultrasonic signal in an intact part of the sintered specimen containing a piece of paper as a simulated defect (Tile 2). The time of flight for the defect-free part of Tile 2 is $T_2 = 2.54$ μs, which is very close to that measured in Tile 1, and for a slightly smaller thickness of the specimen (see Table 2) provides a basically identical value of ultrasonic velocity. The amplitude of the backwall echo in the intact area of Tile 2 is measured at 14.8 V (Fig. 6(a)), and the amplitude of the signal reflected from the paper defect at 2.3 V (Fig. 6(b)). The higher reflection from the defect in Tile 2 is caused by a greater impedance mismatch: the paper defect is burned during sintering and an air void is formed in Tile 2, while the aluminum foil generally melted and diffused in ceramic material in Tile 1.

The A-scan measured in the porous Tile 3 sintered at a lower temperature is shown in Fig. 7. The much greater time-of-flight $T_3 = 3.2$ μs provides a substantially lower velocity of ultrasound due to the porosity of the material (see Table 2).

3.1.2. *Characterization of porosity using material frequency response*

Ultrasonic characterization of porosity can be based on the frequency dependence of attenuation. At low frequencies ($kD < 1$, where k is the wave number and D is the mean size of porous), the ultrasonic attenuation due to scattering (α) is proportional to the fourth power of frequency: $\alpha \sim D^3 f^4$ (Rayleigh scattering). As the frequency increases, the scattering regime changes to stochastic scattering with $\alpha \sim Df^2$, for $kD \geq 1$. The detailed study of frequency dependence $\alpha(f)$ in a

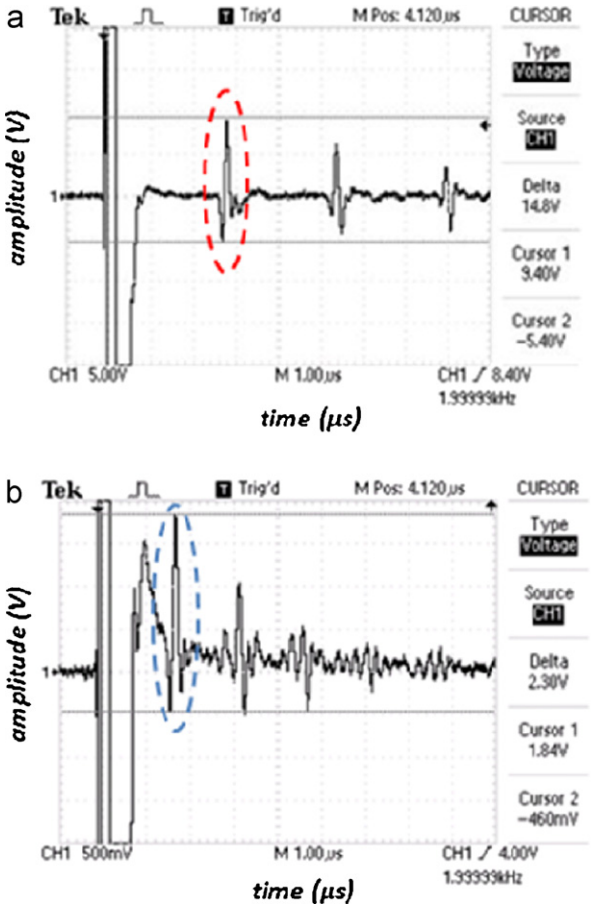

Fig. 6. Measurement of the amplitude of: (a) the backwall echo in intact area, (b) the defect-reflected echo of Tile 2.

wide frequency range, in principle, enables an estimation of the mean size of the pores (D).

A simpler practical approach to the evaluation of material porosity can be based on using conventional medium-band contact ultrasonic transducers. The output amplitude of an ultrasonic transducer is determined by its frequency response and is affected by the frequency dependent attenuation in the material. As a result, the ultrasonic response of a porous material is modified so that the high-frequency end of the frequency response is diminished. For moderately porous materials, an impact of scattering-induced attenuation is not substantial and the material/transducer response exhibits some resonance properties.

A commercial 5 MHz longitudinal wave transducer attached to the surface of the specimens through a couplant layer was used for ultrasound generation/detection in a reflection mode. A short burst (duration of a single period at 5 MHz; amplitude 10–100 V) was generated by a Ritec RAM-5000 Measurement System and applied to the transducer to provide ultrasonic excitation in a wide frequency range determined by the transducer bandwidth. The signal detected was received by an internal Ritec amplifier operating in a frequency sweep mode. In this mode, the receiver central frequency sweeps in a range between 1 and 10 MHz with a step of 1 kHz. The amplitude of the output ultrasonic signal (at a delay time corresponding to certain bottom reflected pulses) after A/D conversion was measured and automatically plotted as a function of the central frequency of the amplifier. This operation is basically equivalent to FFT (within the bandwidth of the transducer) of the signal excited and detected by the ultrasonic transducer after a few round trips in ceramic specimens. The two frequency responses measured for Tiles 1 and 3 are shown in Fig. 8.

The plot for Tile 1 clearly indicates the resonance frequency of the transducer (≈5 MHz), its bandwidth (≈1.5 MHz), and the set of ripples in the area of maximum caused by excitation of the thickness resonance modes. In Tile 3, the low-frequency edge (below ∼4 MHz) closely follows the plot for Tile 1 (Fig. 8). However, the high-frequency end (above ∼4.5 MHz) is damped and exhibits substantially lower amplitude. This is a clear indication of the higher porosity in Tile 3.

3.1.3. Air-coupled C-scan imaging

The air-coupled ultrasound is a well-established technique for noncontact NDT and imaging of defects [8]. In the experiment, weakly focused (focus spot 3–4 mm) 400 kHz air-coupled transducers and a standard scanning table (ISEL-PRO-DIN)

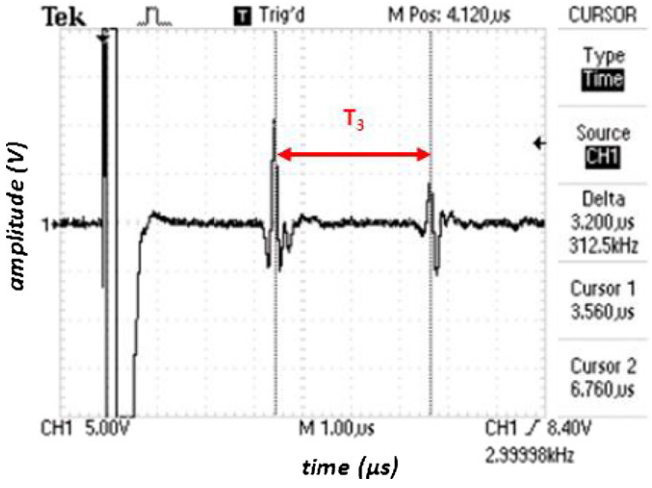

Fig. 7. The time of flight measurement in porous ceramic Tile 3.

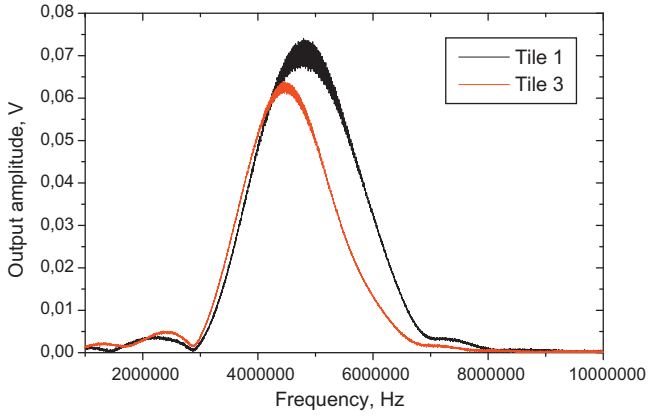

Fig. 8. Damping of high-frequency end of frequency response for porous material (Tile 3).

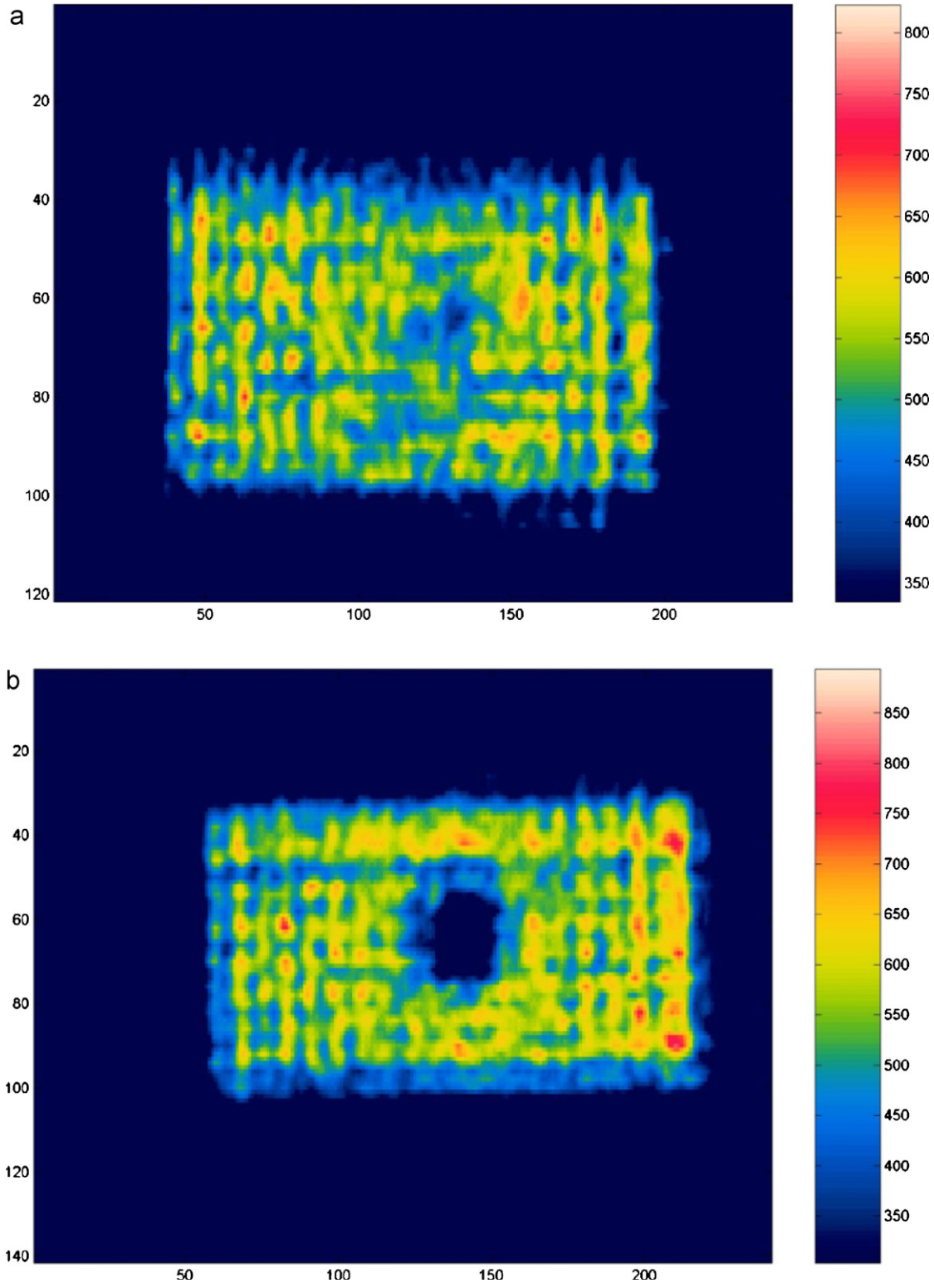

Fig. 9. Color-coded air-coupled images of defects in Tile 1 (a) and Tile 2 (b).

were applied for C-scan imaging defects in ceramic Tiles 1 and 2 in the normal transmission mode [8]. The ultrasonic transmitter was driven by 10-period burst signals of 250 V_{pp} amplitude. The ultrasonic pulse transmitted through the specimen was detected by receiving a transducer and was processed by a data acquisition unit. After A/D conversion, the maximum amplitude of each A-scan was selected, color coded and presented as an amplitude C-scan image.

Fig. 9(a and b) shows the results obtained for Tiles 1 and 2 with simulated defects. The lower amplitude signal in the central area is clearly seen in both images. However, in Tile 2, the contrast of the defect (piece of paper) is much higher than

that for the Al-foil in Tile 2. This confirms the results obtained above in A-scans and indicates considerable infiltration of Al-foil in ceramic material after melting.

4. Conclusions

In this study, it is shown that an A-scan analysis can be used for the detection of different types of defect in ceramic tiles. The presence of a defect in a ceramic tile causes a substantial reduction in the amplitude of the backwall echo and an increase in the signal reflected by material inhomogeneity introduced by the defect. In the sintered sample (Tile 2) with a piece of paper as a simulated defect, a decrease in the backwall echo was observed due to porosity formation in the tile structure during the sintering process. In the sintering process of Tile 1, the aluminum foil melted and infiltrated the tile structure. This diffusion produces a much weaker inhomogeneity in material acoustic impedance and impedes ultrasonic detection of these defects. Nevertheless, both defects in ceramic tiles are detected reliably using an A-scan mode with a contact high-frequency longitudinal wave transducer. It is shown that despite a relatively high impedance of ceramic materials, air-coupled ultrasound can be applied for non-contact detection and the imaging of defects in ceramic tiles.

The results of the study demonstrate that measurements of ultrasonic wave velocity are a reliable tool for the characterization of porosity in ceramic materials. The experiment revealed that less than 5% porosity change in ceramic tiles results in about 20% reduction of ultrasonic wave velocity.

An alternative approach for porosity characterization is based on the frequency dependence of scattering-induced ultrasonic attenuation. To this end, a simple practical technique is proposed which uses the ultrasonic frequency response of the material as an indicator of porosity. An evident damping of the high-frequency end of the frequency response expected, due to scattering by pores, was observed for porous ceramic material. After calibration, this technique can be used for the quantification of porosity, which is an important practical task in the ceramic industry.

Acknowledgement

The financial support from the Anadolu University Scientific Research Project, project 080210, is gratefully acknowledged.

References

[1] A. Vary, Materials Analysis by Ultrasonics: Materials, Ceramics, Composites, Noyes Data Corporation, New Jersey, 1987.
[2] B. Raj, T. Jayakumar, M. Thavasimuthu, Practical Non-destructive Testing, second ed., Alpha Science International Ltd., England, 2002.
[3] K. Kawasaki, inventor, NGK Insulators Ltd., Ultrasonic Testing Method, United States Patent 5,001,674 (1991) March 19.
[4] Metals Handbook, ASM Handbook, Methods of Nondestructive Evaluation, Nondestructive Evaluation and Quality Control, vol. 17, ASM Handbook Committee, The Materials Information Society, American Society for Metals, nineth ed., ASM International, Ohio, 1978–1989, pp. 241–253.
[5] E. Biagi, A. Fort, L. Masotti, L. Ponziani, Ultrasonic high resolution images for defect detection in ceramic materials, Res. Nondestruct. Eval. 6 (1995) 219–226.
[6] J.A. Medding, Nondestructive Evaluation of Zirconium Phosphate Bonded Silicon Radomes [Dissertation], Virginia Polytechnic Institute and State University, Virginia, 1996.
[7] Ultrasonic Non-destructive Testing, The Institution of Metallurgist, The Chameleon Press, London, 1983.
[8] I. Solodov, R. Stössel, G. Buse, Material characterization and NDE using focused slanted transmission mode of air-coupled ultrasound, Res. Nondestruct. Eval. 15 (2004) 1–21.